Electrochemical studies of sulfur-nitrogen compounds. 3. S3N3O-, S3N3O2-, and S4N5O-ions and S4N4O2, S3N2O, Ph2CNSNSO, and S(NSO)2

2 **AUTHORS**, INCLUDING:

Masashi Hojo
Kochi University
114 PUBLICATIONS   **1,549** CITATIONS

Contribution from the Department of Chemistry,
The University of Calgary, Calgary, Alberta, Canada T2N 1N4

Electrochemical Studies of Sulfur–Nitrogen Compounds. 3. $S_3N_3O^-$, $S_3N_3O_2^-$, and $S_4N_5O^-$ Ions and $S_4N_4O_2$, S_3N_2O, $Ph_2CNSNSO$, and $S(NSO)_2$

T. CHIVERS* and M. HOJO

The electrochemical reduction of the anions $S_3N_3O^-$, $S_3N_3O_2^-$, and $S_4N_5O^-$ and the neutral molecules $S_4N_4O_2$, S_3N_2O, $Ph_2CNSNSO$, and $S(NSO)_2$ on mercury and platinum electrodes in CH_3CN–0.1 M R_4NClO_4 (R = Me, Et, *n*-Bu) has been investigated by using voltammetry, coulometry, and UV–visible spectroscopy. The polarographic reduction of the oxygenated derivatives $S_3N_3O^-$, $S_3N_3O_2^-$, $S_4N_5O^-$, and $S_4N_4O_2$ occurs at significantly less negative potentials than the corresponding binary species $S_3N_3^-$, $S_4N_5^-$, or S_4N_4. The coulometric reduction of $S_4N_4O_2$ at –0.5 V (Hg pool) or –0.9 V (Pt gauze) gave a 70% yield of $S_3N_3O_2^-$ (*n* = 0.7). The controlled-potential electrolysis of $S_3N_3O_2^-$ (*n* = 1.3) or $S_4N_5O^-$ (*n* = 4) resulted in breakdown of the ring or cage. The composition of the mixture of products formed on electrolytic reduction of S_3N_2O at –1.15 V on Pt gauze was monitored as a function of electron uptake by UV–visible spectroscopy. The products were $S_3N_3O^-$, S_4N^-, and two other species with absorption maxima at 335 and 405 nm. The reduction of $Ph_2CNSNSO$ at –1.6 V (Hg pool) or –1.75 V (Pt gauze) led to the quantitative formation of $Ph_2CNSSNCPh_2$ and NSO^-. The electrolytically produced NSO^- anion reacts with S_4N_4 to give $S_3N_3O^-$ and with sulfur to give a red species (λ_{max} 496 nm) tentatively identified as S_xNSO^- (*x* = 1 or 2). Electrolysis of $S(NSO)_2$ at the second reduction step (Pt gauze, –2.0 V, *n* > 2) also produced NSO^-, but at the first step (–1.4 V, *n* = 1.0) a species with an absorption maximum at 330 nm was formed.

Introduction

In previous papers in this series we have used electrochemical techniques to probe the redox behavior of both saturated and unsaturated sulfur–nitrogen heterocycles.[1,2] π-Electron-rich rings, e.g. $S_3N_3^-$ and $(Ph_2PN)(SN)_2$, and the related cages S_4N_4 and $S_4N_5^-$ were shown to be good *electron acceptors* as a consequence of the relatively low energies of their LUMOs.[3,4] Electrochemical reduction was also used to generate the recently discovered SN_2^{2-} ion,[5] via exhaustive electrolysis of S_4N_4 at –2.8 V (vs. Ag/0.1 M $AgClO_4$),[1] and a new sulfur–nitrogen anion (λ_{max} 375 nm), tentatively identified as S_2N^-,[2] from S_3N^{-6} or S_4N^-.[7]

We have now investigated the electrochemical reduction of the ions $S_3N_3O^-$ (**1**),[8] $S_3N_3O_2^-$ (**2**),[8] and $S_4N_5O^-$ (**3**)[9] and the neutral molecule $S_4N_4O_2$ (**4**)[10] in order to assess the effect of

exocyclic oxygen substituents on the electron-accepting abilities of the corresponding binary species, $S_3N_3^-$, $S_4N_5^-$, and S_4N_4. We also included S_3N_2O (**5**),[10a,11] $S_3N_2O_2$ (**6**),[12] and $Ph_2CNSNSO$ (**7**)[13] in this study to probe the possible generation of novel S–N–O anions via electrochemical reduction.

The results for the anions **1** and **2** will be discussed first since their electrochemical characterization is necessary for understanding the behavior of the neutral molecules **4** and **5** on electrochemical reduction.

Experimental Section

The compounds $PPN^+S_3N_3O^{-8}$ (PPN = Ph_3PNPPh_3), $PPN^+S_3N_3O_2^-$,[8] *n*-$Bu_4N^+S_4N_5O^-$,[9] $S_4N_4O_2$,[10a] S_3N_2O,[10c] and $Ph_2CNSNSO$[13] were prepared by the literature methods. $S(NSO)_2$ was produced by the reaction of $PPN^+S_3N_3^-$ with $SOCl_2$.[14] $Ph_2CNSSNCPh_2$ was prepared from $Ph_2CNSiMe_3$ and S_2Cl_2 in diethyl ether.[15] The procedures used for purification and drying of acetonitrile[16] and for the preparation and purification of supporting electrolytes[17] have been described elsewhere. $PPN^+ClO_4^-$ was made from commercial PPN^+Cl^- (Alfa) and perchloric acid in a way similar to that of the other supporting electrolytes[17] and recrystallized from ethanol.

Details of the equipment and procedures used for electrochemical and spectrophotometric measurements have been described previously.[1] All potentials are quoted with reference to a Ag/0.1 M $AgClO_4^-$–MeCN electrode.

Results and Discussion

Electrochemical Reductions. The $S_3N_3O^-$ and $S_3N_3O_2^-$ Ions. The anions $S_3N_3^-$ (yellow), $S_3N_3O^-$ (red) (**1**), and $S_3N_3O_2^-$ (purple) (**2**) exhibit intense visible absorption bands at 365,
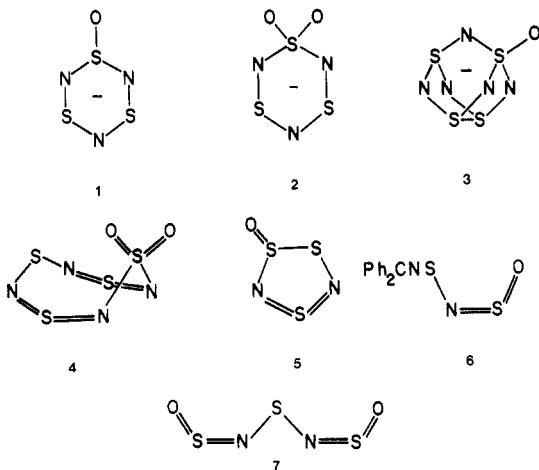
(1) Chivers, T.; Hojo, M. *Inorg. Chem.* **1984**, *23*, 1526.
(2) Chivers, T.; Hojo, M. *Inorg. Chem.* **1984**, *23*, 2738.
(3) Tanaka, K.; Yamabe, T.; Tachibana, A.; Kato, H.; Fukui, K. *J. Phys. Chem.* **1978**, *82*, 2121.
(4) Chivers, T. *Acc. Chem. Res.* **1984**, *17*, 166.
(5) Herberhold, M.; Ehrenreich, W. *Angew. Chem., Int. Ed. Engl.* **1984**, *21*, 633.
(6) Bojes, J.; Chivers, T.; Laidlaw, W. G.; Trsic, M. *J. Am. Chem. Soc.* **1982**, *104*, 4837.
(7) Chivers, T.; Laidlaw, W. G.; Oakley, R. T.; Trsic, M. *J. Am. Chem. Soc.* **1980**, *102*, 5773.
(8) Chivers, T.; Cordes, A. W.; Oakley, R. T.; Pennington, W. T. *Inorg. Chem.* **1983**, *22*, 2429.
(9) (a) Steudel, R. *Z. Naturforsch. B: Anorg. Chem. Org. Chem., Biochem., Biophys., Biol.* **1969**, *24B*, 934. (b) Luger, P.; Bradaczek, H.; Steudel, R. *Chem. Ber.* **1976**, *109*, 3441.

(10) (a) Roesky, H. W.; Schaper, W.; Petersen, O.; Müller, T. *Chem. Ber.* **1977**, *110*, 2695. (b) Jones, P. G.; Pinkert, W.; Sheldrick, G. M. *Acta Crystallogr., Sect. C: Cryst. Struct. Commun.* **1983**, *C39*, 827.
(11) Roesky, H. W.; Kuhn, M.; Bats, J. W. *Chem. Ber.* **1982**, *115*, 3025.
(12) (a) Steudel, R.; Steidel, J.; Rautenberg, N. *Z. Naturforsch., B: Anorg. Chem., Org. Chem.* **1980**, *35B*, 792. (b) MacLean, G.; Passmore, J.; White, P. S.; Banister, A. J.; Durrant, J. A. *Can. J. Chem.* **1981**, *59*, 187.
(13) Chivers, T.; Oakley, R. T.; Pieters, R.; Richardson, J. F. *Can. J. Chem.*, in press.
(14) Chivers, T.; Rao, M. N. S. *Can. J. Chem.* **1983**, *61*, 1957.
(15) Banister, A. J.; Durrant, J. A.; Padley, J. S.; Wade, K. *J. Inorg. Nucl. Chem.* **1979**, *41*, 1415.
(16) Fujinaga, T.; Okazaki, S.; Hojo, M. *J. Electroanal. Chem. Interfacial Electrochem.* **1980**, *44*, 89.
(17) Fujinaga, T.; Okazaki, S.; Hojo, M. *Bull. Inst. Chem. Res., Kyoto Univ.* **1978**, *56*, 139.

Table I. Polarographic Data for the $S_3N_3O_2^-$ and $S_4N_5O^-$ Anions in Acetonitrile at 23 °C

supporting electrolyte[a]	anodic $E_{1/2}$, μA	cathodic $E_{1/2}$, μA		
		$[PPN^+S_3N_3O_2^-] = 0.40$ mM		
Li^+	0.0 (1.45)	−1.14 (3.2)	−1.75 (2.2)	
Na^+	−0.02 (1.7)	−1.24 (2.8)	−1.67 (0.7)	
Me_4N^+	−0.07 (2.0)	−1.40 $(0.4)^b$	−1.60 (1.9)	−1.97 (1.1)
Et_4N^+	−0.06 (1.8)	−1.42 $(0.3)^b$	−1.63 (1.8)	−2.36 (1.0)
Bu_4N^+	−0.05 (1.7)	−1.44 $(0.4)^b$	−1.64 $(1.65)^b$	c
PPN^+	d	−1.46 $(0.4)^b$	−1.54 (1.7)	
		$[PPN^+S_4N_5O^-] = 0.40$ mM		
Li^+		−1.52 (6.4)	−1.96 (3.0)	
Na^+		−1.61 (4.2)		
Me_4N^+		−1.84 (7.9)	−1.99 (3.9)	−2.20 (2.9)
Et_4N^+		−1.91 (5.7)	−2.21 (4.0)	
Bu_4N^+		−1.87 (2.6)	e	
$Bu_4N^{+ f}$		−1.88 (1.3)	−2.49 (1.2)	−2.82 (1.1)

^{a} Concentration of the supporting electrolyte is 0.1 M except for Me_4N^+ and PPN^+ (0.05 M). The potential limit with PPN^+ is −2.4 V vs. Ag/0.1 M $AgClO_4$. ^{b} Prewaves. ^{c} No wave or obscured by PPN^+ wave. ^{d} Not measured. ^{e} Obscured by PPN^+. ^{f} $[Bu_4N^+S_4N_5O^-] = 0.20$ mM.
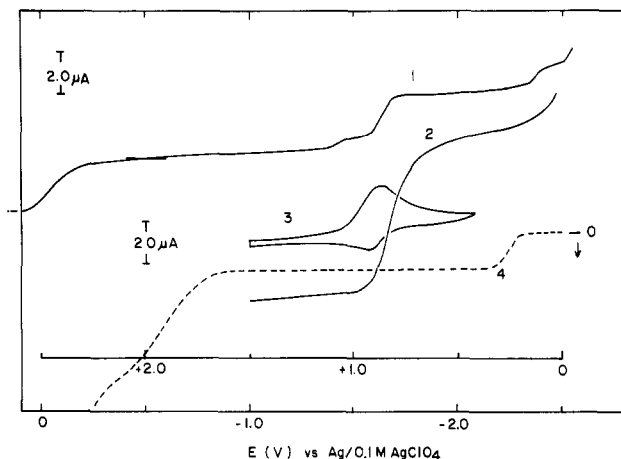

Figure 1. Voltammograms of 0.40 mM $PPN^+S_3N_3O_2^-$ in MeCN containing 0.1 M Et_4NClO_4 at 23 °C: (1) dme; (2) rpe; (3) cyclic voltammogram on Pt electrode, sweep rate 100 mV s^{-1}; (4) oxidation wave on the rpe.

509, and 562 nm, respectively, in methylene dichloride.[8] For $S_3N_3^-$ this band has been assigned to the HOMO (π^*) → LUMO (π^*) transition on the basis of ab initio MO calculations[18] and the MCD spectrum,[19] and a similar assignment has been made for the oxyanions.[8] Thus, the increase in the oxidation state of one of the sulfur atoms in $S_3N_3^-$ by addition of oxygen ligands leads to a substantial decrease in the HOMO–LUMO energy gap.[20] It is not known, however, whether this is due to a stabilization of the LUMO or a destabilization of the HOMO (or a combination of both effects).[8]

The electrochemical results described here suggest that the LUMO is strongly stabilized in the oxyanions compared to $S_3N_3^-$. Specifically, the polarographic reduction of $S_3N_3O^-$ and $S_3N_3O_2^-$ occurs at substantially lower potentials, −1.53 and −1.63 V, respectively (cf. −2.62 V for $S_3N_3^-$ under the same conditions, 0.1 M Et_4NClO_4–MeCN at 23 °C).[1] The
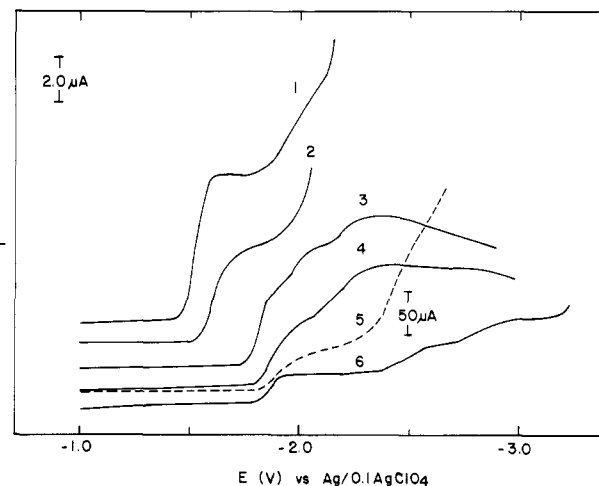

Figure 2. Voltammograms of the $S_4N_5O^-$ anion in MeCN at 23 °C containing $MClO_4$ on dme (except 5): (1) $[PPN^+S_4N_5O^-] = 0.40$ mM, M = Li^+ (0.1 M); (2) $[PPN^+S_4N_5O^-] = 0.40$ mM, M = Na^+ (0.1 M); (3) $[Bu_4N^+S_4N_5O^-] = 0.16$ mM, M = Me_4N^+ (0.05 M); (4) $[Bu_4N^+S_4N_5O^-] = 0.20$ mM, M = Et_4N^+ (0.1 M); (5) case 4, on rpe; (6) $[Bu_4N^+S_4N_5O^-] = 0.20$ mM, M = Bu_4N^+ (0.1 M).

relative ease of reduction of $S_3N_3O^-$ and $S_3N_3O_2^-$ is, however, in the opposite order to that reported for the electronically related molecules $Ph_3P{=}N{-}S_3N_3$ (λ_{max} 488 nm) and $(R_2PN)(SN)_2$ (λ_{max} 550 nm), respectively.[21]

The polarographic data for $PPN^+S_3N_3O_2^-$ are summarized in Table I. In addition to the two cathodic waves at $E_{1/2}$ = −1.63 and −2.36 V, a small prewave was observed at −1.42 V in the presence of 0.1 M Et_4NClO_4–MeCN (Figure 1). The heights of both cathodic waves were a linear function of concentration in the range 0.2–0.9 mM. The first wave was shown to be diffusion controlled by the linear relationship of i_1 with $h^{1/2}$, and the reversibility was high (slope 59 mV). The behavior of the second wave was not straightforward. The wave height decreased compared to that of the first wave as the temperature of the solution was lowered, and at −10 °C the second wave was no longer observed. This suggests that the second wave corresponds to the reduction of a decomposition product formed after the first reduction step.

On the rotating platinum electrode (rpe), the $S_3N_3O_2^-$ ion (0.42 mM) showed a single cathodic wave at $E_{1/2}$ = −1.63 V (slope 92 mV). As indicated in Figure 1, the cyclic voltammogram on a stationary platinum electrode showed only partial reversibility of this process at a sweep rate of 100 mV s^{-1}. At higher sweep rates, however, the value of $(i_p)_a/(i_p)_c$ approached unity. The coulometric reduction of $PPN^+S_3N_3O_2^-$ at −1.8 V gave n values of 1.3–1.4 on both mercury-pool and platinum-gauze electrodes. The initially purple solution became colorless during the electrolysis, and the UV–visible spectrum of the final solution showed no bands other than those due to the PPN^+ cation. Apparently, the product of the first re-

(18) Bojes, J.; Chivers, T.; Laidlaw, W. G.; Trsic, M. *J. Am. Chem. Soc.* **1979**, *101*, 4517.

(19) Waluk, J. W.; Michl, J. *Inorg. Chem.* **1981**, *20*, 963.

(20) As a result of their lower symmetry, compared to $S_3N_3^-$ (D_{3h}), the degeneracy of the HOMO is removed in the oxyanions and a second transition is observed at 340 and 362 nm for $S_3N_3O^-$ and $S_3N_3O_2^-$, respectively.[8]

(21) Liblong, S. W.; Oakley, R. T.; Cordes, A. W.; Noble, M. C. *Can. J. Chem.* **1983**, *61*, 2062. The polarographic reduction potentials of $Ph_3P{=}N{-}S_3N_3$ and $(Ph_2PN)(SN)_2$ are −1.25 and −1.10 V, respectively (vs. SCE in 0.1 M $Bu_4N^+ClO_4^-$–MeCN). These values are consistent with the relative order of LUMO energy levels deduced from calculated (MNDO) HOMO energy levels and experimentally determined HOMO → LUMO transition energies. They are also consistent with the relative rates of cycloaddition reactions of these S–N heterocycles with electron-rich olefins, a process that is dependent primarily on the interaction of the HOMO (olefin) with the LUMO (S–N heterocycle). If the same interaction predominates for sulfur–nitrogen anions, one might expect $S_3N_3O^-$ to react faster than $S_3N_3O_2^-$ with olefins. A preliminary report of the formation of adducts between these oxyanions and norbornadiene has appeared, but details of relative reaction rates were not given: Noble, M. C.; Cordes, A. W.; Oakley, R. T.; Koenig, H. "Abstracts of Papers", 184th National Meeting of the American Chemical Society, Kansas City, MO, Sept 1982; American Chemical Society: Washington, DC, 1982; INOR 87.
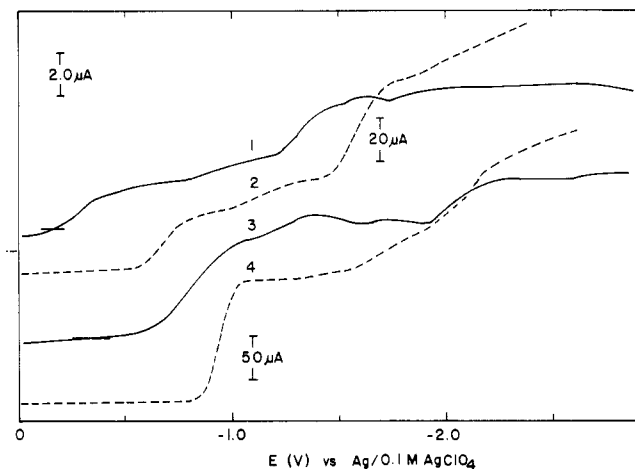
Figure 3. Voltammograms of $S_4N_4O_2$ and S_3N_2O in MeCN containing 0.1 M Et_4NClO_4 at 23 °C: (1) $[S_4N_4O_2]$ = 0.40 mM, on dme; (2) case 1, on rpe; (3) $[S_3N_2O]$ = 0.41 mM, on dme; (4) case 3, on rpe.

duction step decomposes to colorless moieties on the time scale of coulometry ($\sim$15 min).

The $S_4N_5O^-$ Ion. The $S_4N_5O^-$ ion, **3**, is more easily reduced than the $S_4N_5^-$ ion on the dme in the presence of 0.1 M Et_4NClO_4–MeCN. Two cathodic waves, $E_{1/2}$ = –1.91 and –2.21 V, were observed for $S_4N_5O^-$ (cf. $E_{1/2}$ = –2.10 and –2.62 V for $S_4N_5^-$).[1] The voltammetric data for $S_4N_5O^-$ are summarized in Table I and Figure 2. The cation of the supporting electrolyte had a pronounced effect on the polarographic reduction potentials. In the presence of Bu_4NClO_4, the first and second waves were well separated (–1.88 and –2.49 V) and the reversibility of the first wave was enhanced (slope 58 mV; cf. 105 mV for Et_4NClO_4). On the rpe, the $S_4N_5O^-$ ion gave two cathodic waves at –1.92 V (40 μA, 116 mV) and –2.44 V (97.5 μA, 105 mV) in the presence of 0.1 M Et_4NClO_4.

Chemical evidence indicates that the addition of an exocyclic oxygen atom to the $S_4N_5^-$ cage results in a strengthening of the S–N framework. Thus, $S_4N_5^-$ fragments with loss of N_2S to give $S_3N_3^-$ in boiling acetonitrile,[7] while $S_4N_5O^-$ is stable under similar conditions.[22] The electrolysis of $S_4N_5^-$ at the first reduction wave also results in rupture of the cage to give $S_3N_3^-$ with the uptake of 2.5–2.6 electrons.[1] By contrast, the coulometric reduction of $PPN^+S_4N_5O^-$ at –2.05 V in the presence of 0.1 M Bu_4NClO_4 gave n values of 4.8 (Hg electrode) and 4.1 (Pt electrode). The final colorless solution showed a weak absorption band at 350 nm. In the initial stages of the electrolysis on platinum gauze, a pale red color was observed near the electrode surface. This is probably due to the formation of $S_3N_3O^-$ (λ_{max} 509 nm, $E_{1/2}$ = –1.53 V), which would undergo immediate reduction at the potentials used in the electrolysis of $S_4N_5O^-$.

$S_4N_4O_2$. The voltammetric data for $S_4N_4O_2$, **4**, are summarized in Table II and Figure 3. The dioxide is much more easily reduced than S_4N_4 itself. In the presence of 0.1 M Et_4NClO_4, $S_4N_4O_2$ showed two irreversible cathodic waves at $E_{1/2}$ = –0.28 and –1.35 V and an intermediate wave at –0.97 V (cf. S_4N_4; $E_{1/2}$ = –0.93, –2.14, –2.62 V).[1] The height of the first wave was a linear function of concentration and showed diffusion-controlled characteristics. In the case of S_4N_4, we have shown by variable-temperature polarography that the intermediate wave is due to the reduction of $S_4N_4^-$· and the second wave can be attributed to the reduction of $S_3N_3^-$ formed by decomposition of the radical anion.[1] Although $S_4N_4O_2$ is reduced electrolytically to give $S_3N_3O_2^-$ (**2**) (vide infra), the second polarographic wave of **4** does not correspond to the reduction of **2**. Furthermore, the interme-
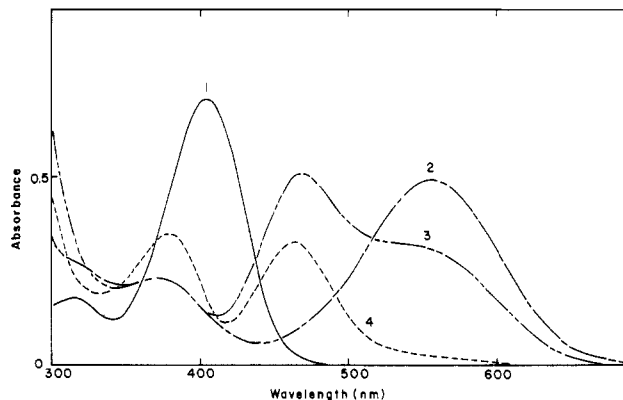
Figure 4. UV–visible spectra of 0.30 mM $S_4N_4O_2$ electrolyzed at –1.7 V on Hg pool in MeCN–0.1 M Et_4NClO_4: (1) $[S_4N_4O_2]$ = 0.40 mM; (2) n = 0.7, after electrolysis; (3) n = 2.0; (4) n = 2.8.
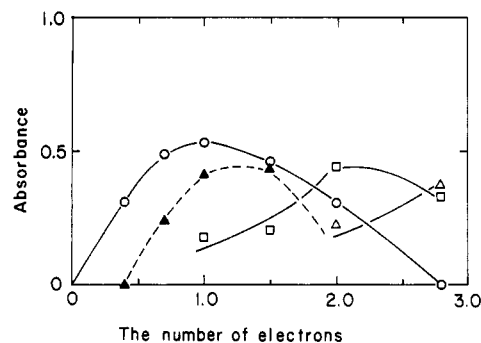

Figure 5. Variation of absorption bands as a function of electron uptake in the electrolysis of $S_4N_4O_2$ (0.30 mM) at –1.7 V on Hg pool, MeCN–0.1 M Et_4NClO_4: (O) 560 nm ($S_3N_3O_2^-$); ($\square$) 465 nm (S_3N^-, corrected for the effect of 560-nm band); ($\triangle$) 375 nm; ($\blacktriangle$) 380–385 nm.

diate wave for **4** was ill-defined and could not be further characterized by variable-temperature experiments. The reduction of $S_4N_4O_2$ occurred at more negative potentials on the rpe than on the dme (Figure 3; $E_{1/2}$ = –0.69 V, 57.5 μA, slope 105 mV; –1.13 V, 22.5 μA; 1.59 V, 105 μA, 113 mV; –1.95 V, 20 μA).

The coulometric reduction of $S_4N_4O_2$ (0.30 mM) at –0.5 V (Hg pool) or –0.9 V (Pt gauze) gave n values of ca. 0.7. The initially yellow solution became purple, and the UV–visible spectrum of the final solution showed bands of approximately equal absorbance at 320, 380, and 560 nm. The band at 560 nm is attributed to the $S_3N_3O_2^-$ ion, which is formed in ca. 70% yield on the basis of its absorbance.[8,23] This assignment was confirmed by voltammetric studies of the final solution (dme and rpe) that revealed anodic and cathodic waves with $E_{1/2}$ values corresponding to those of $S_3N_3O_2^-$.

When the electrolysis was conducted at –1.7 V on a mercury pool, the n value was 2.8 and the solution became orange-yellow via a purple intermediate. The final solution showed two absorption bands at 375 and 465 nm. The latter band can be attributed to the S_3N^- ion.[2,6,24] The polarogram of the solution confirmed the presence of S_3N^-.[2] The 375-nm species has been tentatively identified as S_2N^- in a previous study.[2]

The change in the UV–visible spectrum of an electrolyzed solution of $S_4N_4O_2$ as a function of added electrons is depicted

(22) Chivers, T.; Oakley, R. T.; unpublished results.

(23) The band at 380–385 nm, which grows and decays in a way similar to that of the 560-nm band, can be partly attributed to the second band of $S_3N_3O_2^-$.[20] However, it is clear from the spectra that there is another species, as yet unidentified, contributing to this absorption.

(24) The orange-yellow solution became blue (λ_{max} 580 nm, S_4N^-) after 30 min in the optical cell. This behavior is typical for solutions of S_3N^-.[2,6]

Table II. Polarographic Data for $S_4N_4O_2$ and S_3N_2O in Acetonitrile at 23 °C

supporting electrolyte[a]	cathodic $E_{1/2}$, μA				
		[$S_4N_4O_2$] = 0.40 mM			
Me_4N^+	−0.30 (1.4)	−0.95 (0.6)	−1.32 (2.5)	−2.05 (1.6)	−3.0 (2.6)
Et_4N^+	−0.28 (1.3)	−0.97 (0.5)	−1.35 (2.5)[b]		
Bu_4N^+	−0.28 (1.3)	−0.97 (0.5)	−1.42 (2.25)[b]		
		[S_3N_2O] = 0.41 mM			
Li^+	−0.86 (2.5)[c]	−1.34 (4.2)			
Na^+	−0.82 (4.2)	−1.48 (1.5)			
Me_4N^+	−0.80 (4.2)	−1.90 (2.2)	−2.90 (2.2)		
Et_4N^+	−0.80 (4.2)	−2.05 (1.75)			
Bu_4N^+	−0.88 (3.75)	−2.11 (1.5)			

[a] Concentration of the supporting electrolyte is 0.1 M except for Me_4N^+ (0.05 M). [b] Complicated wave. [c] Accompanied by a prewave at −0.52 V (0.82 μA).

in Figures 4 and 5. The formation of $S_3N_3O_2^-$ reaches a maximum at $n = 1.0$ and is almost quantitative, based on eq 1, at this point. Thus, the electrochemical reduction of $S_4N_4O_2$

$$S_4N_4O_2 + e^- \rightarrow S_3N_3O_2^- + \text{"SN"} \qquad (1)$$
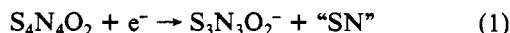
resembles that of S_4N_4 in that the addition of one electron results in a ring contraction to give a six-membered ring. It should also be noted that the nucleophilic reduction of S_4N_4[25] and $S_4N_4O_2$[8] with azide ion gives the same ring-contraction products. Gleiter has suggested that $S_4N_4O_2$ can be regarded as a 10-π-electron NSNSNSN unit linked into a ring by the SO_2 group.[26] The LUMO of $S_4N_4O_2$ will, therefore, be antibonding with respect to S–N linkages, and consequently, addition of an electron is expected to lead to ring opening. The open-chain intermediates formed in this way apparently recyclize to give six-membered rings.

Beyond $n = 1.0$, the amount of $S_3N_3O_2^-$ decreases and the yields of S_3N^- and the 375-nm species increase. It should be recalled, however, that the coulometric reduction of the $S_3N_3O_2^-$ itself at −1.8 V (Hg pool or Pt gauze) does *not* produce S_3N^- or the 375-nm species. Thus, it appears that the fragment "SN" (eq 1) plays an important role in the formation of S_3N^- in the electrolysis of $S_4N_4O_2$.

S_3N_2O. The voltammetric data for S_3N_2O (5) are summarized in Table II and Figure 3. The polarographic reduction occurred in two steps at −0.80 and −2.05 V in the presence of 0.1 M Et_4NClO_4. The heights of both waves were a linear function of concentration (0.2–0.8 mM) and were diffusion controlled, but totally irreversible. On the rpe, three cathodic waves were observed at −0.94 V (135 μA, slope 58 mV), −1.70 V (32.5 μA, 190 mV), and −2.05 V (52.5 μA, 160 mV).

Gleiter et al. have pointed out that the bonding in the SNSN segment of the ring in 5 can be regarded as butadiene-like with the important difference that three, rather than two, of the π-MOs are occupied.[27] An additional electron will, therefore, occupy a π-MO that is very strongly antibonding with respect to the S–N framework, and rupture of the ring can be anticipated. The behavior of S_3N_2O on electrolytic reduction is quite different on a mercury-pool electrode compared to on platinum gauze. In the former case, at −1.15 V the initially yellow solution became pale purple and then red. The n value was 1.0, and HgS was formed during the electrolysis.[28] The final solution had absorption bands at 340 and 505 nm characteristic of the $S_3N_3O^-$ ion (Figure 6),[8,20] and the polarogram gave a cathodic wave at −1.54 V (cf. −1.53 V for
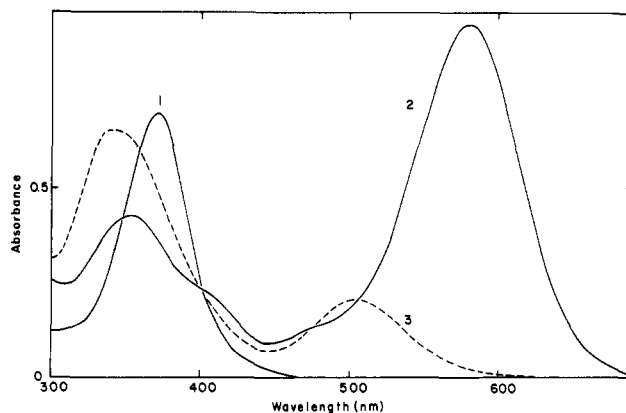
(25) Bojes, J.; Chivers, T. *Inorg. Chem.* **1978**, *17*, 318.
(26) Gleiter, R. *Angew. Chem., Int. Ed. Engl.* **1981**, *20*, 444.
(27) Gleiter, R.; Bartetzko, R.; Hofmann, P. *Z. Naturforsch., B: Anorg. Chem. Org. Chem.* **1980**, *35B*, 1166.
(28) No HgS was formed when S_3N_2O was stirred on a mercury pool for 30 min. Presumably, the HgS formed in the electrolysis results from the reaction of mercury with one of the reduction products.

Figure 6. UV–visible spectra of 0.30 mM S_3N_2O electrolyzed at −1.15 V, MeCN–0.1 M Et_4NCl_4: (1) [S_3N_2O] = 0.41 mM; (2) $n = 1.3$, after electrolysis on Pt gauze; (3) $n = 1.0$, after electrolysis on Hg pool.
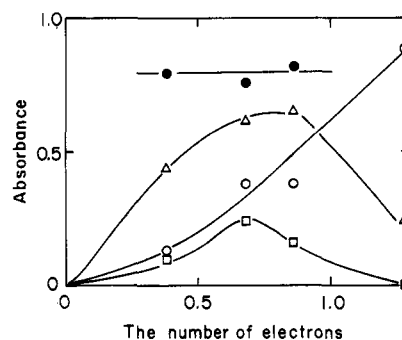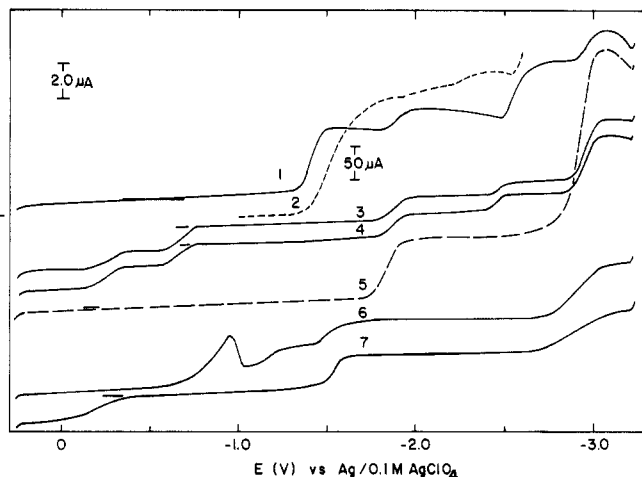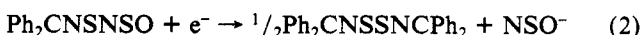

Figure 7. Variation of absorption bands as a function of electron uptake in the electrolysis of 0.30 mM S_3N_2O at −1.15 V on Pt gauze, MeCN–0.1 M Et_4NClO_4: (●) 335 nm; (△) 405 nm; (○) 580 nm (S_4N^-); (□) 505 nm ($S_3N_3O^-$).

$S_3N_3O^-$). From the intensity of the 505-nm band, the yield of $S_3N_3O^-$ was ca. 25% (based on oxygen).

When the electrolysis was carried out on a platinum-gauze electrode, the final color of the solution was blue for an n value of 1.3 (Figure 6). The absorption spectrum revealed the formation of S_4N^- (λ_{max} 580 nm, ca. 5 × 10^{-5} M)[7] from S_3N_2O (3 × 10^{-4} M). Unidentified bands were also observed at 335 and 405 nm. The formation of products was monitored as a function of electron uptake (Figure 7). At $n = 0.4$, the purple color was found to be due to a combination of S_4N^- (λ_{max} 580 nm) and $S_3N_3O^-$ (λ_{max} 505 nm), and at this stage, the behavior is similar to that observed for the Hg-pool electrode. In the latter case, however, the S_4N^- ion disappeared as the n value increased whereas the concentration of S_4N^- continued to increase on the Pt-gauze electrode. The concentration of $S_3N_3O^-$ reached a maximum at $n = 0.7$ and was undetectable

Figure 8. Voltammograms for Ph$_2$CNSNSO, Ph$_2$CNSSNCPh$_2$, and S(NSO)$_2$ in MeCN–0.1 M Et$_4$NClO$_4$ at 23 °C on dme (except 2): (1) [Ph$_2$CNSNSO] = 0.4 mM; (2) case 1, on rpe; (3) electrolysis of Ph$_2$CNSNSO (0.27 mM) at –1.75 V on Pt gauze; (4) electrolysis of Ph$_2$CNSNSO (0.27 mM) at –1.6 V on Hg pool; (5) [Ph$_2$CNSSNCPh$_2$] = 0.40 mM; (6) [S(NSO)$_2$] = 0.21 mM; (7) electrolysis of S(NSO)$_2$ (0.20 mM) at –1.4 V on Pt gauze.

at n = 1.3. In this connection, it should also be mentioned that the current–time curve for electrolysis on Pt gauze began to increase just after n = 0.7, reached a maximum at 0.85, and then decreased logarithmically. The current maximum was not observed on the mercury-pool electrode, but similar maxima have been observed in previous studies.[2,29,30] For n values 0.4–0.9 the unidentified species with bands at 335 and 405 nm were predominant.

Ph$_2$CNSNSO. As shown in Figure 8, Ph$_2$CNSNSO (6) (0.40 mM) gave four cathodic waves on the dme at –1.39 V (3.4 μA, 65 mV), –1.86 V (1.2 μA, 84 mV), –2.55 V (2.8 μA, 84 mV), and –2.95 V (3.15 μA, 60 mV) in 0.1 M Et$_4$NClO$_4$–MeCN at 23 °C. The heights of all four waves were a linear function of concentration in the range 0.2–0.8 mM. The third and fourth waves were shown to be diffusion controlled by the linear relationship of i_1 with $h^{1/2}$. A linear relationship was also observed for the first wave, but the intercept had a negative value. The second wave was under kinetic control. At –15 °C, this wave disappeared completely and the height of the fourth wave became smaller relative to the first and third. On the rpe a single cathodic wave was observed at –1.53 V (150 μA, 150 mV) and an anodic wave at +1.33 V (135 μA, 100 mV) for Ph$_2$CNSNSO (0.40 mM) in 0.1 M Et$_4$NClO$_4$–MeCN. Cyclic voltammograms on a stationary Pt electrode showed the cathodic process to be irreversible.

Coulometric reductions of Ph$_2$CNSNSO (0.27 mM) on Hg-pool or Pt-gauze electrodes at –1.6 or –1.75 V, respectively, both gave n values of 1.0. The electrolyzed solutions exhibited a strong absorption band at 300 nm (cf. Ph$_2$CNSNSO; λ_{max} 370 nm).[13] The polarograms of these solutions showed two anodic waves at –0.24 V (1.2 μA) and –0.68 V (1.35 μA) and three cathodic waves at –1.87 V (1.2 μA), –2.46 V (0.5 μA), and –2.95 V (3.1 μA). The cathodic waves and the UV absorption band at 300 nm were shown to be identical with those obtained for Ph$_2$CNSSNCPh$_2$ (prepared from Ph$_2$CNSiMe$_3$ and S$_2$Cl$_2$), which was formed quantitatively according to eq 2.

$$\text{Ph}_2\text{CNSNSO} + \text{e}^- \rightarrow {}^1/_2\text{Ph}_2\text{CNSSNCPh}_2 + \text{NSO}^- \quad (2)$$

(29) Fujinaga, T.; Kuwamoto, T.; Okazaki, S.; Hojo, M. *Bull. Chem. Soc. Jpn.* **1980**, *53*, 2851.
(30) Hojo, M. *Bull. Chem. Soc. Jpn.* **1980**, *53*, 2856.

The anion NSO$^-$ has been prepared recently, but only infrared spectral data were reported.[31] The addition of S$_4$N$_4$ to the pale brown electrolyzed solution above produced a red solution (λ_{max} 505 nm) of S$_3$N$_3$O$^-$ according to eq 3. The anodic waves at –0.24 and –0.68 V can therefore be attributed to the NSO$^-$ anion. The electrolytically produced NSO$^-$ anion

$$\text{NSO}^- + {}^1/_2\text{S}_4\text{N}_4 \rightarrow \text{S}_3\text{N}_3\text{O}^- \quad (3)$$
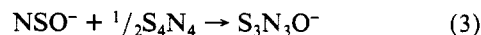
also reacted with elemental sulfur to give a red solution, λ_{max} 496 nm. The nonexistence of an absorption band at 340 nm[20] or a polarographic wave at –1.53 V demonstrated that this red species is not S$_3$N$_3$O$^-$. In order to determine the composition of this new red species, we titrated solutions of the NSO$^-$ anion with a solution of elemental sulfur in acetonitrile. The absorption band at 496 nm reached a maximum for an NSO$^-$:S° ratio of 1:1, and the polarogram of the solution showed the presence of unreacted sulfur for a 1:2 molar ratio, suggesting that the red species is SNSO$^-$.[32]

S(NSO)$_2$. As shown in Figure 8, S(NSO)$_2$ (7) (0.21 mM) in 0.1 M Et$_4$NClO$_4$–MeCN gave three cathodic waves on the dme. The first wave was poorly defined, but the second and third waves at $E_{1/2}$ = –1.50 and –2.90 V were well behaved. On the rpe, two waves were observed at –1.21 and –1.62 V. Coulometric reduction at –2.0 V on Pt gauze consumed more than 2 electrons/mol of S(NSO)$_2$. The electrolyzed solution was almost colorless and exhibited no absorption maxima in the UV–visible spectrum. The polarogram of this solution gave two anodic waves at potentials close to those of NSO$^-$ (vide supra) and an irreversible cathodic wave at –2.94 V. The presence of the NSO$^-$ ion was confirmed by the formation of S$_3$N$_3$O$^-$ (λ_{max} 505 nm) on addition of S$_4$N$_4$ to the electrolyzed solution, which also produced a small amount of S$_4$N$^-$ (λ_{max} 580 nm).[7]

Electrolysis of S(NSO)$_2$ (0.20 mM) on a Pt-gauze electrode at the first reduction step (–1.4 V) resulted in the uptake of one electron. The electrolyzed solution exhibited a strong absorption band at 330 nm. The same species was also produced when a solution of S(NSO)$_2$ in MeCN (1.0 mM, λ_{max} 365 nm) was allowed to stand at 23 °C for 3–4 h, presumably as a result of nucleophilic reduction. The polarogram of the electrolyzed solution is displayed in Figure 8. The anion NSO$^-$ is not present in this solution since addition of S$_4$N$_4$ does not produce S$_3$N$_3$O$^-$.

Summary and Conclusion

The presence of exocyclic oxygen substituents enhances the electron-acceptor properties of sulfur–nitrogen rings, presumably as a result of a lowering of the LUMO energy levels. The electrochemical reduction of S$_4$N$_4$O$_2$ to S$_3$N$_3$O$_2^-$ provides another example of the parallel behavior exhibited by sulfur–nitrogen compounds on electrochemical or nucleophilic reduction. The reactions of electrolytically produced NSO$^-$ with S$_4$N$_4$ to produce S$_3$N$_3$O$^-$ or with sulfur to give S$_x$NSO$^-$ (x = 1 or 2) suggest the possibility of using the NSO$^-$ ion as a template to construct novel S–N–O anions. We are actively pursuing the chemical synthesis of such anions from NSO$^-$.

(31) Armitage, D. A.; Brand, J. C. *J. Chem. Soc., Chem. Commun.* **1979**, 1078.
(32) Cordes, A. W.; Koenig, H.; Noble, M. C.; Oakley, R. T. *Inorg. Chem.* **1983**, *22*, 3375. π-Donor ligands have been shown to induce a large bathochromic shift on the π* → π* transition energy of the X–SNSS chromophore. On this basis the derivatives Ph$_2$CNSNSO (λ_{max} 370 nm) and OSNSNSO (λ_{max} 365 nm) might be expected to have a lower energy transition than the anion SNSO$^-$.[13] Consequently, we do not rule out the possibility that the 496-nm species is SSNSO$^-$ (cf. SSNSS$^-$; λ_{max} 580 nm),[7] formed by disproportionation of SNSO$^-$ (cf. SNSS$^-$).[2,6]

for the preparation of $S_4N_4O_2$.

Mass Spectrometric Investigation of Silver Ion Promoted C–C Bond Scission
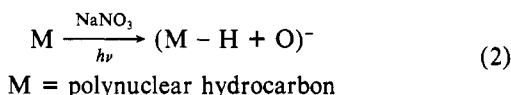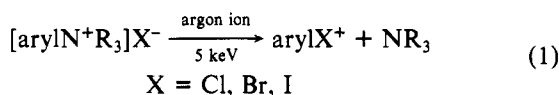
K. L. BUSCH,[†‡] R. G. COOKS,*[‡] R. A. WALTON,*[‡] and K. V. WOOD[§]

Both the secondary ion mass spectra (SIMS) and the electron ionization mass spectra of silver salts of acetic acid, propionic acid, and benzoic acid exhibit positive ions associated with C–C bond scission. A formal relationship exists with the classical Hünsdiecker reaction in which the essential step is thermal decarboxylation. In both types of mass spectrometric experiments the observation of cationized forms of the hydrocarbon products of the Hünsdiecker reaction strengthens the analogy and suggests that ion beam impact as well as thermal heating can initiate cleavage reactions of silver salts in the solid state. There is also a gas-phase contribution to the C–C scissions observed in the mass spectrometer. This was demonstrated explicitly by mass selection of silver-containing ions and characterization of the fragments formed by collisional activation. Cluster ions C_2A^+, where C is the cation and A the anion, for example (Ag₂propionate)⁺, fragment to give C–C cleavage products $AgCO_2^+$ and $AgCO^+$, as well as Ag_2OH^+, Ag_2H^+, and Ag_2^+. Metal clusters are particularly prominent in SIMS spectra, which contain abundant Ag_3^+ ions not seen at all in the electron ionization mass spectra. Studies of ions such as Ag_2X^+ (X = H, O, OH, CH₃, CH₃CO₂, and CH₃CH₂CO₂) by tandem mass spectrometry reveal that most dissociate to the silver dimer ion Ag_2^+. However, Ag_2H^+ and Ag_2OH^+ do not do so and therefore appear not to contain metal–metal bonds. Parent and daughter spectra were used to obtain information that allows structures for these unusual ions to be formulated.

Introduction

Parellels between reactions occurring in solution and in the mass spectrometer provide insights into chemistry in both milieus. This comparison has been made for unimolecular reactions encountered in electron ionization mass spectrometery[1,2] and for bimolecular ion/molecule reactions carried out under chemical ionization conditions[3–5] in ion cyclotron resonance,[6–8] and in drift tube instruments.[9,10] Striking similarities as well as sharp contrasts have been reported. With the advent of desorption ionization procedures such as secondary ion mass spectrometry (SIMS),[11–13] new types of mass spectrometric reactions are being encountered and comparisons with solution chemistry should continue to be fruitful. This is a new area of activity typified by observations such as the apparent nucleophilic substitution (eq 1) seen in secondary ion

$$[arylN^+R_3]X^- \xrightarrow[\text{5 keV}]{\text{argon ion}} arylX^+ + NR_3 \quad (1)$$

$$X = Cl, Br, I$$

$$M \xrightarrow[h\nu]{\text{NaNO}_3} (M - H + O)^- \quad (2)$$

$$M = \text{polynuclear hydrocarbon}$$

mass spectrometry[14] and the oxygen displacement reaction (eq 2) observed in laser desorption of polynuclear aromatic hydrocarbons.[15] In some cases reactions accompanying desorption complicate the analysis, as in the examination of thiamine hydrochloride from glycerol matrix, where hydrogenolysis apparently occurs.[16]

The Hünsdiecker reaction[17] is a thermal decarboxylation; the prototype (eq 3) involves the silver salt of the acid in the presence of halogen and mercuric oxide.

$$RCO_2Ag + Br_2 \xrightarrow[\text{HgO}]{\Delta} RBr + CO_2 + AgBr \quad (3)$$

A free-radical mechanism is usually invoked, and the formation of the alkane, RR, as a secondary product supports this postulate. Our interests in the nature of the fragmentation reactions occurring in secondary ion mass spectrometry (SIMS),[18] in organic reactions at silver,[19] and in the fragmentation of silver-containing compounds[20] led us to examine the SIMS spectra of silver salts of organic acids. Ions corresponding to C–C bond cleavage were observed, and this suggested that possible parallels with the Hünsdiecker reaction should be explored. This was done by generating some of the

(1) Levsen, K.; Schwarz, H. *Mass Spectrom. Rev.* **1981**, *2*, 77.
(2) Ramana, D. V.; Gruzmacher, H. F. *Org. Mass Spectrom.* **1981**, *16*, 228.
(3) Glish, G. L.; Cooks, R. G. *J. Am. Chem. Soc.* **1978**, *100*, 6720.
(4) Burinsky, D. J.; Cooks, R. G. *J. Org. Chem.* **1982**, *47*, 4864.
(5) Maquestiau, A.; Van Haverbeke, Y.; deMayer, C.; Duthoit, C.; Meyrant, P.; Flammang, R. *Nouv. J. Chim.* **1979**, *3*, 517.
(6) Bartmess, J. E.; McIver, R. T., Jr. In M. J. Bowers (Ed.), "Gas Phase Ion Chemistry"; Bowers, M. J., Ed.; Academic Press: New York, 1979; Vol. 2, Chapter 11.
(7) Carlin, T. J.; Freiser, B. S. *Anal. Chem.* **1983**, *55*, 571.
(8) Lehman, T. A.; Bursey, M. M. "Ion Cyclotron Resonance Spectrometry"; Wiley-Interscience: New York, 1976.
(9) DePuy, C. H.; Grabowski, J. J.; Bierbaum, V. M. *Science (Washington, D.C.)* **1982**, *218*, 955.
(10) Squires, R. R.; Bierbaum, V. M.; Grabowski, J. J.; DePuy, C. H. *J. Am. Chem. Soc.* **1983**, *105*, 5185.
(11) Benninghoven, A.; Sichtermann, W. *Org. Mass Spectrom.* **1977**, *12*, 595.
(12) Busch, K. L.; Cooks, R. G. *Science (Washington, D.C.)* **1982**, *218*, 247.
(13) Colton, R. J.; Murphy, J. S.; Wyatt, J. R.; DeCorpo, J. J. *Surf. Sci.* **1979**, *84*, 235.
(14) Day, R. J.; Unger, S. E.; Cooks, R. G. *Anal. Chem.* **1980**, *52*, 557.
(15) Balasanmugan, K.; Viswanadham, S. K.; Hercules, D. M. *Anal. Chem.* **1983**, *55*, 2424.
(16) Glish, G. L.; Todd, P. J.; Busch, K. L.; Cooks, R. G. *Int. J. Mass Spectrom. Ion Phys.*, in press.
(17) Wilson, C. V. *Org. React. (N.Y.)* **1957**, *9*, 332.
(18) Unger, S. E.; Day, R. J.; Cooks, R. G. *Int. J. Mass Spectrom. Ion Phys.* **1981**, *39*, 231.
(19) Unger, S. E.; Cooks, R. G.; Steinmetz, B. J.; Delgass, W. N. *Surf. Sci.* **1982**, *116*, L211.
(20) Pierce, J. L.; Busch, K. L.; Cooks, R. G.; Walton, R. A. *Inorg. Chem.* **1983**, *22*, 2492.

†Present address: Department of Chemistry, Indiana University, Bloomington, IN 47405.
‡Department of Chemistry.
§Engine Fuels Laboratory, Interdisciplinary Engineering Institute.